REGULAR PAPER

DOI: 10.1007/s12541-017-0187-0
ISSN 2234-7593 (Print) / 2005-4602 (Online)

Simulation Analysis of Potential Energy Recovery System of Hydraulic Hybrid Excavator

Peng-Yu Zhao[1], **Ying-Long Chen**[1], and **Hua Zhou**[1,#]

1 State Key Laboratory of Fluid Power and Mechatronic Systems, Zhejiang University, Hangzhou 310027, China
Corresponding Author / E-mail: hzhou@sfp.zju.edu.cn, TEL: +86-571-87951271-6223, FAX: +86-571-87951646

KEYWORDS: Hybrid power, Excavator, Hydraulic, Potential energy recovery

A new hydraulic hybrid excavator potential energy recovery system is proposed in this paper. The energy recovery system uses three-chamber cylinders (TCCs) and accumulators to recover potential energy during work cycle. Within this structure, there is no throttle valve in the primary loop, and the recovered energy is stored in the form of hydraulic energy. Hence, energy loss of throttle valve and energy conversion process are avoided, and energy efficiency is improved. The mathematical model is established to analyze dynamic and energy recovery characteristics. From simulation analysis, the usage of accumulators and TCC influences the dynamic response and stability. The increase of accumulator volume weakens the control performance but heightens the stability. When the cross sectional area of the TCC increases, the control performance of the system are improved. In addition, the maximum power and energy consumption of pumps and engine with different accumulator volumes and different TCC diameters are obtained. Also, the maximum power and energy consumption of each pump and engine in different working conditions are obtained and compared with those without potential energy recovery system. According to the comparison, the potential energy recovery system can reduce the maximum power and energy of engine by 50%.

Manuscript received: April 11, 2016 / Revised: June 19, 2017 / Accepted: July 19, 2017

NOMENCLATURE

A_{11} = cross sectional area of boom cylinder counterweight chamber
A_{12} = cross sectional area of boom cylinder chamber without piston rod
A_{13} = cross sectional area of boom cylinder chamber with piston rod
B_1 = viscous damping coefficient of boom cylinder
C_{11} = external leakage coefficient of counterweight chamber
C_{12} = internal leakage coefficient between counterweight chamber and the chamber with piston rod
C_{13} = internal leakage coefficient between the chambers with and without piston rod
C_{14} = external leakage coefficient of the chamber without piston rod
C_{15} = external leakage coefficient of the chamber with piston rod
C_e = equivalent viscous damping of engine
C_{1P} = sum of internal and external leakage coefficient of pump
C_{ve} = compression loss coefficient of pump
C_{vs} = structure leakage coefficient of pump
D_1 = viscous damping coefficient of boom
D_p = displacement of pump
d_p = diameter of pipe
F_1 = output force of boom cylinder
F_2 = output force of arm cylinder
F_3 = output force of bucket cylinder
f_1 = friction force of boom cylinder
F_{load} = weight of load
F_{G1} = weight of boom
F_{G2} = weight of arm
F_{G3} = weight of bucket and load
G_1 = barycenter of boom
G_2 = barycenter of arm
G_3 = barycenter of bucket
J_{11} = rotational inertia of boom rotating around point B
J_{12} = rotational inertia of arm rotating around point B
J_{13} = rotational inertia of bucket and load rotating around point B
J_e = equivalent rotational inertia of engine
J_p = equivalent rotational inertia of pump

k_{p1}, k_{p2}, k_{p3} = mechanical loss coefficient of pump
L = hydraulic inductance of accumulator
L_{01} = length of boom cylinder when piston rod retracts
L_{x1} = displacement of boom cylinder piston rod
L_{x2} = displacement of arm cylinder piston rod and
L_{x3} = displacement of bucket cylinder piston rod
l_p = length of pipe connected to accumulator
M_e = fuel efficiency
m_1 = mass of boom cylinder piston rod
m_f = fuel consumption of engine
n = polytropic exponent
P_e = output power of engine
P_p = power of pump
p_a = pressure of accumulator
p_{a_line} = pressure of pipe
p_{a1} = outlet pressures of boom accumulator
p_{a2} = outlet pressures of arm accumulator
p_{a3} = outlet pressures of bucket accumulator
P_{11} = pressure of boom cylinder counterweight chamber
P_{12} = pressure of boom cylinder chamber without piston rod
P_{13} = pressure of boom cylinder chamber with piston rod
p_{1p} = outlet pressures of boom pump
p_{2p} = outlet pressures of arm pump
p_{3p} = outlet pressures of bucket pump
p_a = pressure of accumulator
P_{1P} = pressure of pump outlet
Δp_p = pressure difference between high pressure chamber and low pressure chamber of pump
Q_1 = flow of closed pump control system
q_a = flow rate of accumulator
q_{v1} = flow rate of boom closed pump control system
q_{v2} = flow rate of arm closed pump control system
q_{v3} = flow rate of bucket closed pump control system
q_{vp} = flow rate of pump
Q_{1a} = flow rate that the boom accumulator provides
Δq_{v11} = leakage rate of counterweight chamber
Δq_{v12} = leakage rate of chambers with and without piston rod
Δq_{vp} = flow rate loss of pump
R = hydraulic resistance of accumulator
T_1 = the friction torque of boom
T_e = output torque of engine
T_{el} = load torque
T_p = torque of pump
T_{p1} = needed torque of boom pump
T_{p2} = needed torque of arm pump
T_{p3} = needed torque of bucket pump
ΔT_p = torque loss of pump
V_{11} = equivalent volume of boom counterweight chamber
V_{12} = volume of the chamber without piston rod
V_{13} = volume of the chamber with piston rod
V_a = volume of accumulator
V_p = volume of pump outlet
v_1 = piston rod speed of boom
X_{G1} = horizontal ordinate of G_1
X_{G2} = horizontal ordinate of G_2
X_{G3} = horizontal ordinate of G_3
α_{com} = target location of opening degree of throttle
α_e = opening degree of throttle of engine
β_1 = concluded angle between boom cylinder and boom (line BC)
β_e = effective bulk modulus of hydraulic oil
β_p = viscous damping coefficient of pump
η_{vp} = volume efficiency of pump
θ_1 = included angle between line BC and the horizontal direction
η = dynamic viscosity of oil
ρ = density of oil
φ_1 = included angle between line AB and the horizontal direction
ω_e = rotate speed of engine
ω_p = rotate speed of pump

1. Introduction

Nowadays, engineering machineries are playing significant roles in construction, transportation, mining and other fields. Generally, engineering machineries have high power, large fuel consumption and exhaust emission. However, the shortage of hydrocarbon resources and environmental problems have gradually become a heated issue during the past few years. Efforts to reduce power, fuel consumption and exhaust emission are being made to reduce size and weight, as well as to develop direct injection gasoline and diesel engine technologies to improve fuel efficiency.[1] In the area of transmission technology, the research core is focused on hybrid technology and fuel cell technology. Since fuel cell technology is still in its early development stages, hybrid technology seem to be the most viable solution.[2] So the energy recovery of engineering mechanical using hybrid technology is of great significance for alleviating resource and environmental problems.

As one of the main engineering mechanicals, excavator has typical working condition characteristics. For instance, the average movement velocity of excavator is low, the operation period is short with frequent start-stops and reciprocating motion. The potential energy is usually converted to heat energy and wasted when the mechanical arms move downwards. What's worse, this will cause system heating and shorten the life of components. Meanwhile, the load of excavator mechanical arms is gravity load with a great deal of recyclable energy. For the above reasons, excavator becomes the focus in the research of energy recovery.

At present, the development tendency of hydraulic hybrid machineries includes several directions. Some researchers focuse on using pump controlled system to replace valve controlled system. Team of Professor Monika Ivantysynova from Purdue University[3,4] studied on hydraulic hybrid system architecture for multi-actuator displacement controlled systems. From the experiments on 5-ton excavator, the system reduces fuel consumption by 40%, and decreases the engine size by 50%. Also, Ken Sugimura et al from RWTH Aachen University,[5] Mikko Erkkilä et

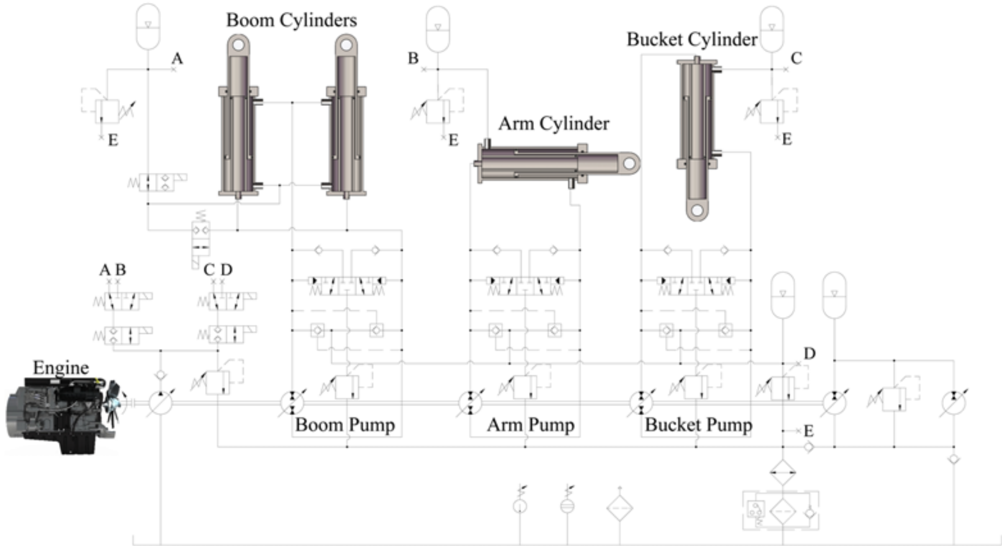

Fig. 1 Schematic diagram of potential energy recovery system

al from Hydac International GmbH,[6] Seppo Tikkanen et al from Tampere University of Technology[7] and other researchers also raised several hydraulic hybrid energy recovery systems for excavators with pump controlled systems. The pump controlled system makes the flow rate of pump outlet to meet the need of movements by changing the displacement or rotate speed of the pump. Thus the throttle loss of hydraulic valve is avoided, which raises the system efficiency.[8] Some researchers preferred secondary regulation hydraulic system. As an example, Jihai Jiang and Wei Shen et al. from Harbin Institute of Technology[9-11] proposed a hydraulic hybrid excavator based on constant pressure rail and design control strategies. The system uses hydraulic transformers to drive the mechanical arms and recover the potential energy together with hydraulic accumulators. The system reduces fuel consumption by around 1/3. What's more, Shuwen Lin et al. from Fuzhou University,[12] Peter Achten et al from Innas BV[13] and others also research on this direction with fruitful achievements. Secondary regulation hydraulic systems eliminate the throttle loss to increase energy efficiency. There are no interferences between loads and the controllability is better, which brings a broad development prospect.[14] Some other researchers developed new complex system and components to recover potential energy of excavator mechanical arms. Yang Xiao from Zhejiang University[15] proposed a flow coupling hydraulic hybrid excavator and designed a control strategy, which improved the energy recovery rate by 10.1%. Torben Andersen et al. from Aalborg University[16] Mikko Huova[17] and Stauch[18] et al from Tampere University of Technology also showed great interests in complex system and components. The systems reduce energy conversion components between energy sources and actuators to decrease the loss of energy. However, the manufacture of complex components is difficult, which puts forward a higher request to control strategy.

In the aspect of energy recovery and storage, since the energy density is not large enough, a majority of hydraulic hybrid excavators use battery or super capacitance to store energy. Mostly, the electric system provides 5-10% installed engine power,[19] and hydraulic system provides peak power at the same time. However, the energy conversion between electric system and hydraulic system is usually accompanied by great energy loss. Therefore, developing a new potential energy recovery system becomes the key to reduce the energy loss during transformation and conversion among hydraulic system and to increase the efficiency.

In this paper, a new hydraulic hybrid excavator potential energy recovery system based on complex cylinder is proposed. The mathematical model of each part is built and the dynamic response is analyzed. Also, simulation model is carried out and simulation result is analyzed.

2. Working Principle

Based on the analysis of hydraulic hybrid excavator potential energy recovery system, a new potential energy recovery system applicable to hydraulic hybrid excavator is proposed. The schematic diagram is shown in Fig. 1. The actuators of the specific system include a boom, an arm and a bucket, which are driven by boom cylinders, arm cylinder and bucket cylinder, respectively.

In the proposed hydraulic hybrid potential energy recovery system, the mechanical arms are driven by three-chamber cylinders (TCCs). The recovered potential energy is stored in hydraulic accumulators. A TCC comprises three chambers, including a chamber with piston rod, a chamber without piston rod and a counterweight chamber, shown in Fig. 2. The volumes of the three chambers are equal. The counterweight chamber is connected to the accumulator, and the chambers with and without piston rod are connected to inlet and outlet of the variable pump, forming closed pump control systems. The movements of the mechanical arms is controlled by the closed pump control system.

During normal work cycle of the hydraulic hybrid excavator, the variable pump charges the chamber with piston rod or the chamber without piston rod according to the control signal, which drives the TCC to retract or to extend, respectively. The accumulator provides high pressure oil to the counterweight chamber. The counterweight chamber provides average value of load force. When the piston rod extends, the

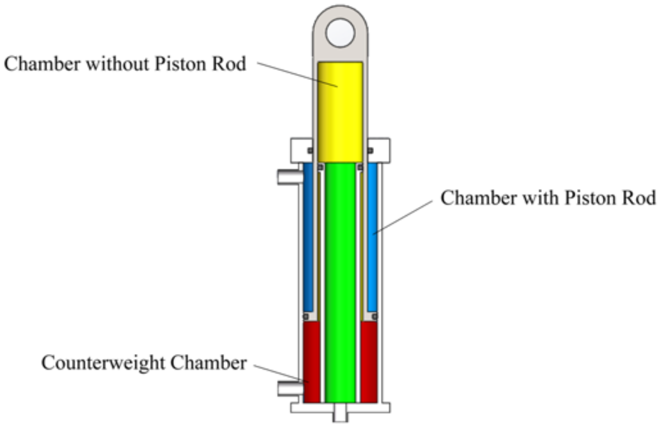

Fig. 2 Schematic diagram of TCC

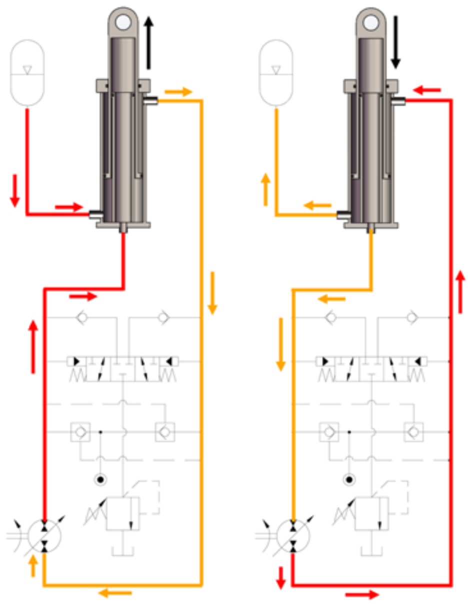

(a) Piston rod extends (b) Piston rod retracts

Fig. 3 Movements of piston rod

variable pump charges the chamber without piston rod, and the accumulator charges the counterweight chamber, as shown in Fig. 3(a). On the contrary, when the piston rod retracts, the variable pump charges the chamber with piston rod, and the counterweight chamber charges the accumulator, as shown in Fig. 3(b). In this way, the potential energy is recovered and stored in the accumulator in the form of pressure energy.

The TCCs in the system is driven by closed pump control system. The variable pumps are connected to the engine through power trains. The engine provides needed power and maintains constant rotate speed. The flow rate of the pump outlet is adjusted by the variable pump displacement to meet the need of mechanical arms' movement. In this approach, the throttling loss of throttle valve is avoided, which increases the system efficiency. Since there are no energy dissipating components between energy sources and actuators, using a variable pump to control the movements of a cylinder becomes the most efficient way at present.[7] During the potential energy recover process, the gravitational potential energy of loads and mechanical arms are converted into the pressure energy of the counterweight chambers, and then transformed into pressure energy of the accumulators. There is no need to convert or transform the pressure energy into other forms any further. However, as a contrast, traditional hydraulic hybrid excavators converted pressure energy into electric energy through throttle valves, hydraulic motors, electric generators, super capacitances, batteries and so on, generally. Compared with traditional ones, the proposed potential recovery system simplifies the process of energy transfer, and reduces energy loss.

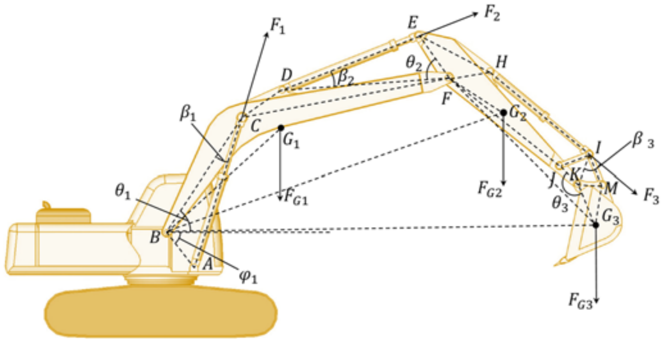

Fig. 4 Force diagram of boom

3. Mathematical Model

From Fig. 1, we can get that the basic principles of the boom, arm and bucket potential energy recovery hydraulic circuits are the same. Hence, the mathematical model of each circuit are almost the same. Therefore, in this paper, only boom mathematical model is established as an example.

3.1 Mathematical model of load

For the proposed hydraulic hybrid excavator potential recovery system, the force diagram of boom is shown in Fig. 4.

We assume that point B is the origin of coordinates, consider the horizontal direction as X axes and the vertical direction as Y axes to establish coordinate.

The kinetic equation of the boom is shown as the following equation.

$$\begin{aligned}&(J_{11}+J_{12}+J_{13})\frac{\mathrm{d}^2\theta_1}{\mathrm{d}t^2} = \\ &F_1 L_{BC}\sin\beta_1 - F_{G1}X_{G1} - F_{G2}X_{G2} - F_{G3}X_{G3} - D_1\frac{\mathrm{d}\theta_1}{\mathrm{d}t} - T_1\end{aligned} \tag{1}$$

According to cosine law, the geometrical relationships of the boom and the cylinders can be described using the following equations.

$$\theta_1 = \arccos\left[\frac{L_{AB}^2 + L_{BC}^2 - (L_{01}+L_{x1})^2}{2L_{AB}L_{BC}}\right] - \varphi_1 \tag{2}$$

$$\beta_1 = \arccos\left[\frac{L_{BC}^2 + (L_{01}+L_{x1})^2 - L_{AB}^2}{2L_{BC}(L_{01}+L_{x1})}\right] \tag{3}$$

Where φ_1 is a constant value.

The speed of the boom cylinder piston rod is calculated as follows.

$$v_1 = \frac{\mathrm{d}L_{x1}}{\mathrm{d}t} \tag{4}$$

3.2 Mathematical model of engine

The fuel consumption model is shown in the following equation.

$$m_f = \int T_e M_e\left(T_e, \alpha_e\right)\omega_e\left(T_e, \alpha_e\right)\mathrm{d}t \tag{5}$$

The output torque of the engine is calculated in the following equation.[21]

$$T_e = \frac{\pi}{30}J_e\frac{\mathrm{d}\omega_e}{\mathrm{d}t} + \frac{\pi}{30}C_e\omega_e + T_{el} \tag{6}$$

The output torque of the engine is determined by the engine performance and the opening degree of throttle.

In the proposed hydraulic hybrid system, the rotate speed of the engine is constant, which means:

$$\frac{\mathrm{d}\omega_e}{\mathrm{d}t}=0 \tag{7}$$

Then the output torque of the engine can be rewritten as:

$$T_e = \frac{\pi}{30}C_e\omega_e + T_{el} \tag{8}$$

The output power of the engine is expressed as follows.

$$P_e = T_e\omega_e \tag{9}$$

The dynamic response of the engine governor can be regarded as a first order inertia process, and the mathematical model can be written as the following equation.[22]

$$\tau\frac{\mathrm{d}\alpha_e}{\mathrm{d}t} + k\alpha_e = \alpha_{com} \tag{10}$$

Where τ and k are constants.

3.3 Mathematical model of pump

The input power of the pump is shown in the following equation.

$$P_p = T_p\omega_p \tag{11}$$

The torque of the pump is shown as follows.[23]

$$T_p = J_p\frac{\mathrm{d}\omega_p}{\mathrm{d}t} + \beta_p\omega_p + \Delta p_p D_p \tag{12}$$

The flow rate of the pump is calculated in the following equation.

$$q_{vp} = \eta_{vp}D_p\omega_p \tag{13}$$

The continuity equation of the variable displacement piston pump can be obtained as the following equation.[24]

$$\frac{V_p}{\beta_e}\frac{\mathrm{d}p_p}{\mathrm{d}t} = q_{vp} - \frac{\omega_p D_p}{2\pi} - C_p\Delta p_p \tag{14}$$

3.4 Mathematical model of TCC

The kinetic equation of the boom cylinder can be shown as follows.

$$m_1\frac{\mathrm{d}v_1}{\mathrm{d}t} = F_1 + p_{11}A_{11} + p_{12}A_{12} - p_{13}A_{13} - B_1v_1 - F_{f1} \tag{15}$$

The continuity equation of the boom cylinder counterweight chamber can be expressed as:

$$\frac{V_{11}}{\beta_e}\frac{\mathrm{d}p_{11}}{\mathrm{d}t} = A_{11}v_1 - q_{va1} - C_{11}p_{11} - C_{12}\left(p_{11} - p_{12}\right) - C_{13}\left(p_{11} - p_{13}\right) \tag{16}$$

Where V_{11} includes the volume of the boom cylinder counterweight chamber, accumulator, and connecting pipe between the boom cylinder and the accumulator.

The continuity equation of the boom cylinder chamber without piston rod can be shown as the following equation.

$$\frac{V_{12}}{\beta_e}\frac{\mathrm{d}p_{12}}{\mathrm{d}t} = A_{12}v_1 - q_{v1} - C_{14}p_{12} - C_{12}\left(p_{12} - p_{11}\right) \tag{17}$$

The continuity equation of the boom cylinder chamber with piston rod can be obtained as follows.

$$\frac{V_{13}}{\beta_e}\frac{\mathrm{d}p_{13}}{\mathrm{d}t} = q_{v1} - A_{13}v_1 - C_{15}p_{13} - C_{13}\left(p_{13} - p_{11}\right) \tag{18}$$

3.5 Mathematical model of accumulator

According to Boyle's law, the thermodynamic equation of the accumulator is shown in the following equation.

$$p_aV_a^n = \text{const.} \tag{19}$$

Where n is determined by the working condition of the accumulator.

The kinematical equation can be written as follows.[25]

$$L\frac{\mathrm{d}q_a}{\mathrm{d}t} + Rq_a = p_{a\_line} - p_a \tag{20}$$

Where

$$L=\rho\frac{4l_p}{\pi d_p^2} \tag{21}$$

And

$$R=\frac{128\mu l_p}{\pi d_p^4} \tag{22}$$

According to the equations above, the equilibrium equation can be written as the following equation.

$$\rho\frac{4l_p}{\pi d_p^2}\frac{\mathrm{d}V_a^2}{\mathrm{d}^2t} + \frac{128\mu l_p}{\pi d_p^4}\frac{\mathrm{d}V_a}{\mathrm{d}t} = p_{a\_line} - p_a \tag{23}$$

3.6 Energy loss

The energy loss of the process from the TCC counterweight chamber to the accumulator is calculated in the following equation.

$$P_{loss1} = p_{11}\Delta q_{v11} \tag{24}$$

The energy loss of the process from the TCC to the pump is calculated

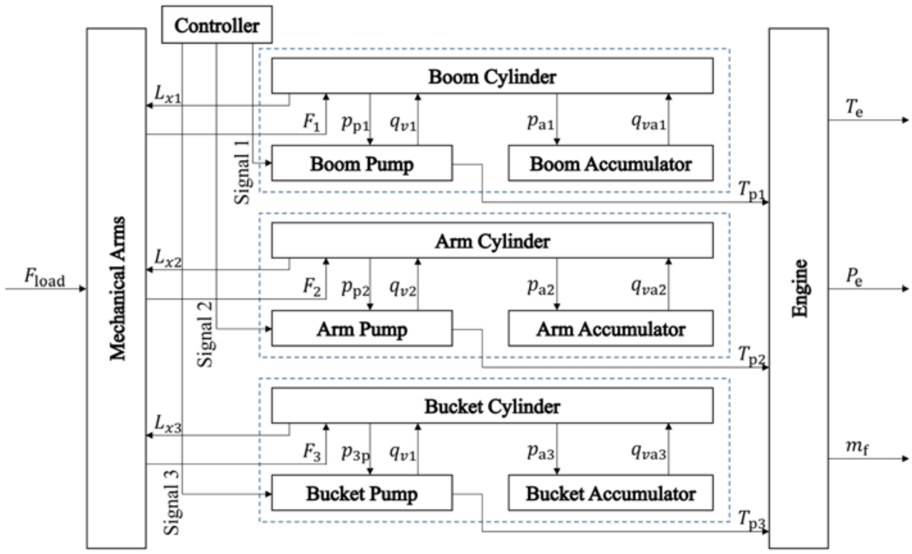

Fig. 5 Principle diagram of simulation model

in the following equation.

$$P_{loss2} = p_{12}\Delta q_{v12} \tag{25}$$

The mechanical energy loss of the pump is calculated as follows.

$$P_{pm} = \Delta T_p \omega_p = k_{p1}\Delta p_p \omega_p + k_{p2} q_{vp} \omega_p^3 + k_{p3} q_{vp} \Delta p_p \tag{26}$$

The volume energy loss of pump is calculated as follows.

$$P_{pv} = \Delta q_{vp} \cdot p_p = C_{vs}\Delta p_p \cdot p_p + C_{ve} q_{vp} \omega_p \Delta p_p \cdot p_p \tag{27}$$

We can obtain the total energy loss of the pump as:

$$P_{loss3} = P_{pm} + P_{pv} \tag{28}$$

With the development of sealing material and process, the leakage of cylinders and piston pumps has been decreased greatly. Also, from parameter identification we can get that the values of coefficients k_{p1}, k_{p2} and k_{p3} are small with magnitude orders of 10^{-2}~10^{-4}. So the energy loss of the potential energy recovery system is low.

4. Parameter Matching

The objective of parameter matching is to choose the volume of accumulators and diameter of TCCs according to the dynamic characteristics and energy recovery characteristics of the excavator. The selection of parameters makes the system to achieve a better and more balanced performance between control performance and energy recovery rate, and minimize the geometric dimensioning and weight of actuators at the same time.

In order to analyze dynamic characteristics and energy recovery efficiency of the hydraulic hybrid excavator potential energy recovery system, simulation model is established in MATLAB/Simulink. The principle diagram of the simulation model is shown in Fig. 5.

Parameters of variable pumps and engine are shown in Table 1.

Table 1 Simulation parameter of main components

Parameter	Specification
Variable pump	
Boom pump displacement	100 mL/r
Arm pump displacement	100 mL/r
Bucket pump displacement	50 mL/r
Maximum working pressure	35 MPa
Engine	
Rating power	122 kW (2000 rpm)
Maximum torque	650 Nm (1500 rpm)
Rotate speed setting value	2000 rpm

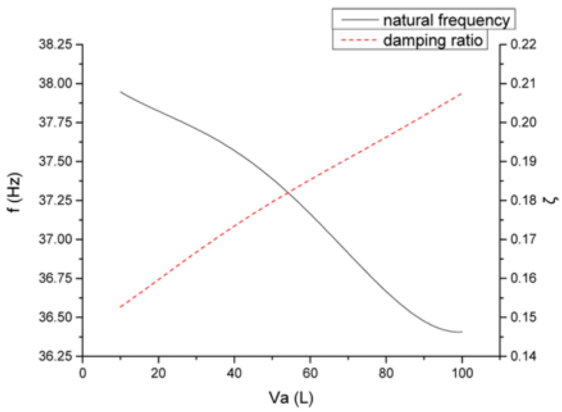

Fig. 6 Natural frequency and damping ratio of TCC piston rod with different accumulator volumes

4.1 Dynamic characteristics

In order to analyze how the parameters of the accumulators and the TCCs influence the dynamic characteristics of the potential energy recovery system, simulations on the velocity of the cylinder piston rod

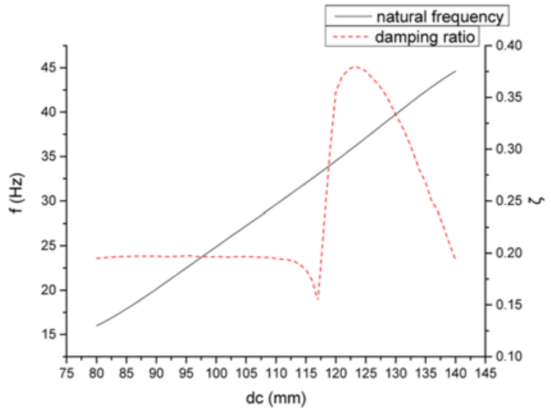

Fig. 7 Natural frequency and damping ratio of TCC piston rod with different cylinder diameters

are carried out with different accumulator volumes and different cylinder diameters. Also, since the basic principles of the boom, arm and bucket potential energy recovery hydraulic circuits are the same, the simulation is made only on the boom circuit as an example. Fig. 6 shows variation of natural frequency (f) and damping ratio (ζ) of the boom TCC piston rod with different accumulator volumes.

From Fig. 6, when the volume of the accumulator is 10 L, the natural frequency of the system is 37.9 Hz. As the accumulator volume gets larger, the natural frequency of the TCC piston rod becomes smaller. When the volume of the accumulator is 100 L, the natural frequency is 36.4 Hz. Hence, with the increase of the accumulator volume, the natural frequency decreases, which weakens the control performance of the system. On the other hand, when the accumulator volume is 10 L, the damping ratio of the TCC piston rod is 0.15. As the accumulator volume gets larger, the damping ratio of the TCC piston rod increases. When the accumulator volume is 100 L, the damping ratio of the TCC piston rod is 0.21. Hence, with the increase of the accumulator volume, the damping ratio increases, which heightens the stability of the system.

Fig. 7 shows the variation of natural frequency and damping ratio of the TCC piston rod with different diameters of chamber without piston rod.

From Fig. 7, when the diameter of the chamber without piston rod is 80 mm, the natural frequency of the TCC piston rod is 15.9 Hz. When the diameter of the chamber without piston rod gets larger, the natural frequency of the TCC piston rod increases. When the diameter of the chamber without piston rod is 140 mm, the natural frequency of the system is 44.4 Hz. Hence, with the increase of diameter of the chamber without piston rod, the cross sectional area of the complex cylinder increases, and the natural frequency increases, which strengthen the control performance of the system. On the other hand, in the range of 80~117 mm, when the diameter of the chamber without piston rod increases, the damping ratio gets smaller. When the diameter of the chamber without piston rod is larger than 117 mm, the ratio rate increases first, and then decreases with the increase of the diameter of chamber without piston rod. When the diameter of the chamber without piston rod is 123 mm, the damping ratio of the TCC piston rod gets the maximum value, which is 0.38.

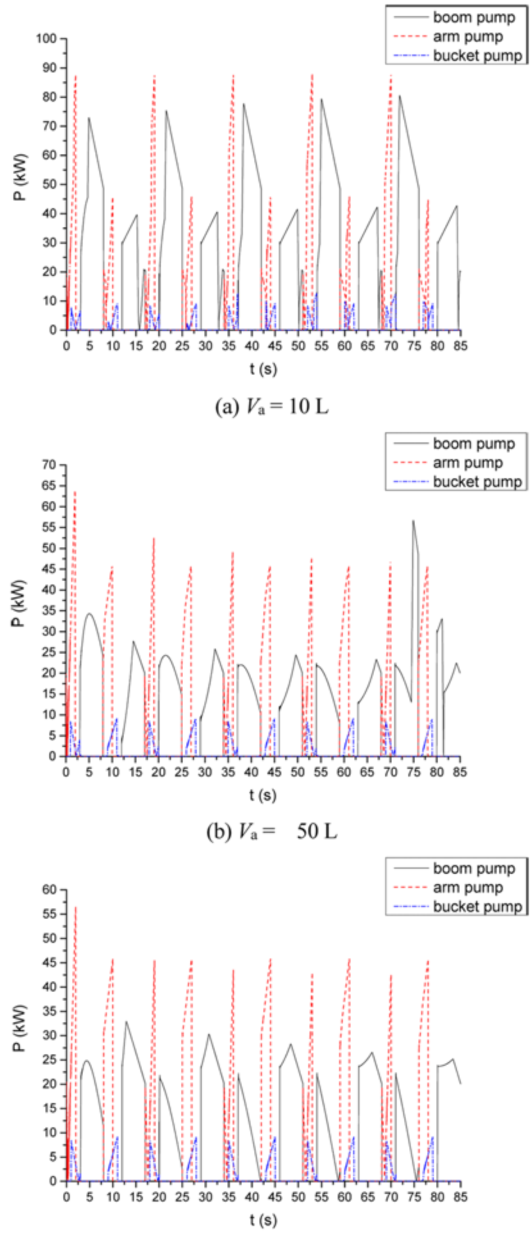

(a) V_a = 10 L

(b) V_a = 50 L

(c) V_a = 100 L

Fig. 8 Power of pumps with different accumulator volumes

Meanwhile, the increase of accumulator volume and TCC cross sectional area makes it more difficult to install the components since the weight and volume become larger. Therefore, the selection of the accumulator volume and the TCC diameter should take all the factors into account, including control performance, stability, install size, total weight and so on.

4.2 Energy recovery characteristics

In order to analyze the energy recovery characteristics of the potential recovery system with different accumulator volumes, constant load is chosen as the typical working condition. The power of each pump with the accumulator volumes of 10 L, 50 L and 100 L are shown in Fig. 8.

The engine power with the accumulator volumes of 10 L, 50 L and 100 L is shown in Fig. 9.

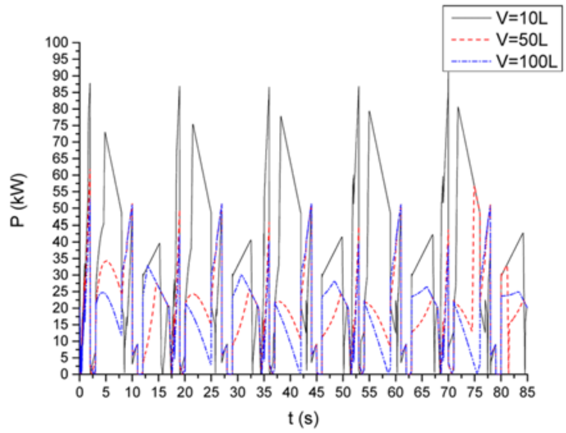

Fig. 9 Engine power with different accumulator volumes

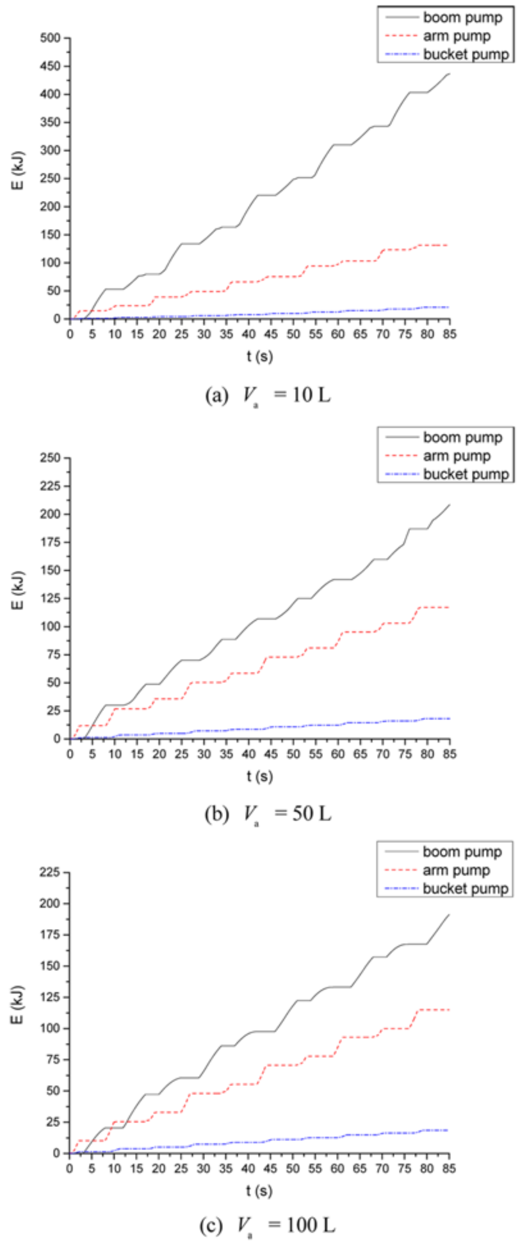

Fig. 10 Energy consumption of pumps with different accumulator volumes

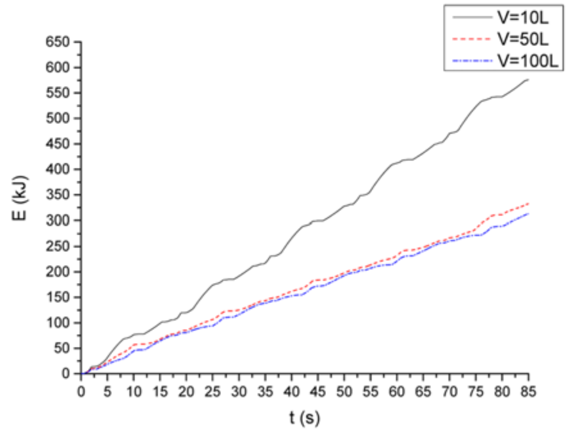

Fig. 11 Energy consumption of engine with different accumulator volumes

Table 2 Maximum power of the pumps and the engine with different accumulator volumes (Unit: kW)

	V_a = 10 L	V_a = 50 L	V_a = 100 L
Boom pump	80.6	56.8	33.0
Arm pump	88.0	63.9	56.6
Bucket pump	12.8	9.2	9.2
Engine	91.1	67.1	63.2

Table 3 Energy consumption of the pumps and the engine with different accumulator volumes (Unit: kJ)

	V_a = 10 L	V_a = 50 L	V_a = 100 L
Boom pump	436	208	191
Arm pump	131	117	115
Bucket pump	21	18	18
Engine	576	333	313

And the energy consumption of each pump with different accumulator volumes is shown in Fig. 10.

Energy consumption of the engine with accumulator volumes of 10 L, 50 L and 100 L is shown in Fig. 11.

According to the simulation results, the maximum power of each pump and the engine with different accumulator volumes is summarized in Table 2.

From Table 2 we can get that when the volume of the accumulators increases, the maximum power of the pumps and the engine decreases. Also, the smaller the volumes of accumulators are, the more obvious the effect is to decrease the maximum power when the values of volume change are the same.

The energy consumption of each pump and the engine with different accumulator volumes is summarized in Table 3.

From Table 3 we can get that when the volume of accumulators increases, the energy consumption of the pumps and the engine decreases. However, when the volume of the accumulators gets larger, the recovered energy of unit volume is lower. This will lead to less obvious contribute to energy recovery efficiency when the accumulator volume increases. Meanwhile, the increase of accumulator volume will occupy more space in the excavator, and brings difficulty in installation. As a result, the volume of the accumulators should be chosen reasonably

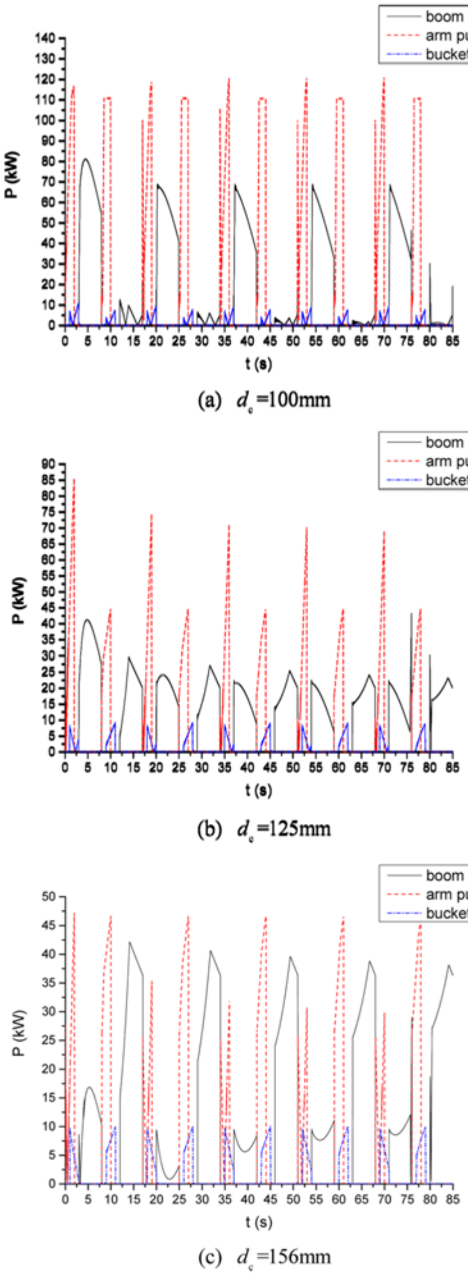

(a) d_c=100mm

(b) d_c=125mm

(c) d_c=156mm

Fig. 12 Power of pumps with different TCC diameters

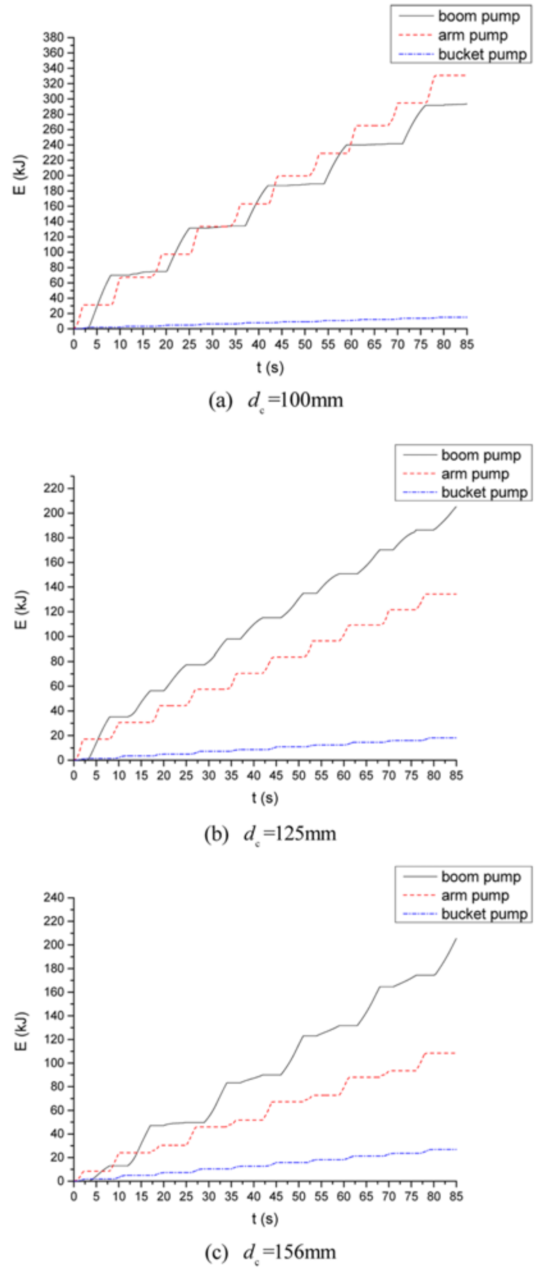

(a) d_c=100mm

(b) d_c=125mm

(c) d_c=156mm

Fig. 14 Energy consumption of pumps with different TCC diameters

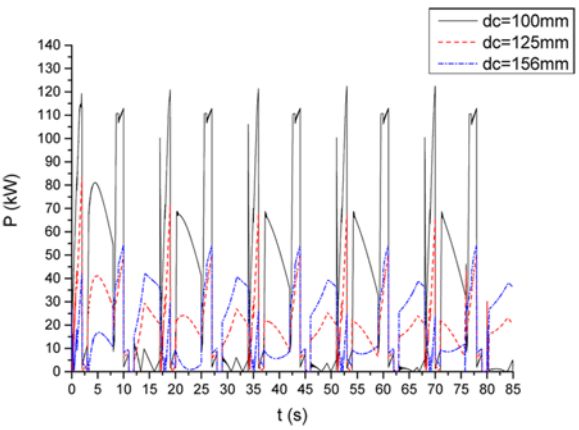

Fig. 13 Power of engine with different TCC diameters

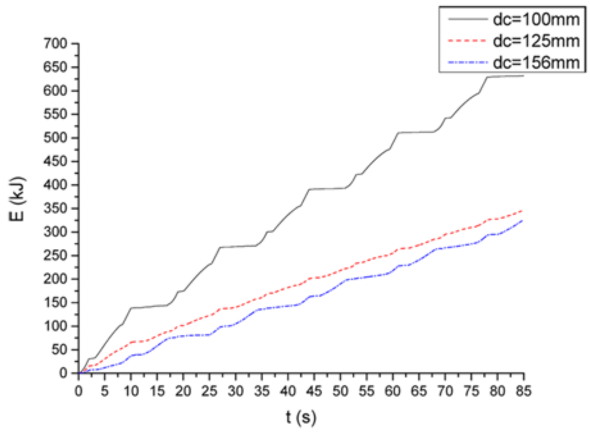

Fig. 15 Energy consumption of engine with different TCC diameters

Table 4 Maximum power of the pumps and the engine with different TCC diameters (Unit: kW)

	d_c = 100 mm	d_c = 125 mm	d_c = 156 mm
Boom pump	81.1	43.2	42.2
Arm pump	121.2	85.6	47.2
Bucket pump	11.1	9.2	10.1
Engine	122.5	88.7	54.5

Table 5 Energy consumption of the pumps and the engine with different TCC diameters (Unit: kJ)

	d_c = 100 mm	d_c = 125 mm	d_c = 156 mm
Boom pump	294	205	205
Arm pump	331	134	108
Bucket pump	15	18	26
Engine	632	346	326

Table 6 Parameters of TCCs

	D_c / mm	d_c / mm	L_c / mm	V_a / L
Boom	177	125	1160	70
Arm	198	140	1350	50
Bucket	177	125	970	40

based on installation space, engine power and expect energy recovery efficiency.

Meanwhile, the energy recovery characteristics of the potential recovery system with different TCC diameters is analyzed. The power of each pump with the TCC diameters of 100 mm, 125 mm and 156 mm are shown in Fig. 12.

The power of the engine with TCC diameters of 100 mm, 125 mm and 156 mm is shown in Fig. 13.

The energy consumption of each pump with different TCC diameters is shown in Fig. 14.

The energy consumption of the engine with different TCC diameters is shown in Fig. 15.

According to the simulation results, the maximum power of each pump and the engine with different TCC diameters is summarized in Table 4.

From Table 4 we can get that when the diameters of TCCs increase, the maximum power of the boom, arm pumps and the engine decreases. However, the difference of the bucket pump maximum power is little. The maximum power of the bucket pump when the diameter of the bucket TCC is 156 mm is larger than that of 125 mm.

The energy consumption of each pump and the engine with different TCC diameters is summarized in Table 5.

From Table 5 we can get that when the TCC diameter increases, the energy consumption of pumps and engine decreases. However, when the diameter of TCCs gets larger, the recovered energy is lower. Also, the energy consumption of bucket pump when bucket TCC diameter is 156 mm is larger than that of 125 mm. This is because when the TCC diameter is large enough, the increment of needed flow rate is large, which will increase the resistance loss of pipeline and other energy loss. But the pressure decrease due to the TCC cross sectional area increase is limited. Then the pressure and the flow rate of pump outlet increase, which increases the power and energy consumption of pumps

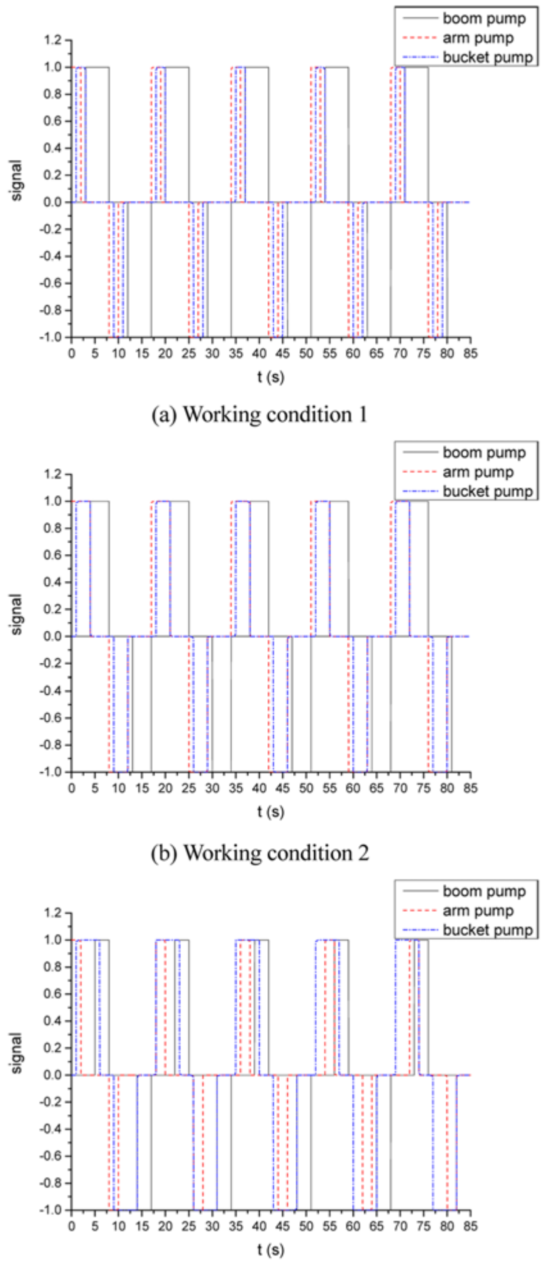

(a) Working condition 1

(b) Working condition 2

(c) Working condition 3

Fig. 16 Control signals of pump displacement in different working conditions

and engine. Meanwhile, the increase of TCC diameter will add the weight of the excavator, and makes the TCCs more difficult to install on the excavator. So the diameter of TCCs should be chosen reasonably based on load and engine power.

According to dynamic characteristic and energy recovery characteristics of the energy recovery system, taking installation space, engine power and load of excavator into account, the parameters of TCCs and accumulator volume are selected, which are shown in Table 6.

Where D_c is the diameter of the chamber with piston rod, d_c is the diameter of the chamber without piston rod, and L_c is the stroke of the piston rod.

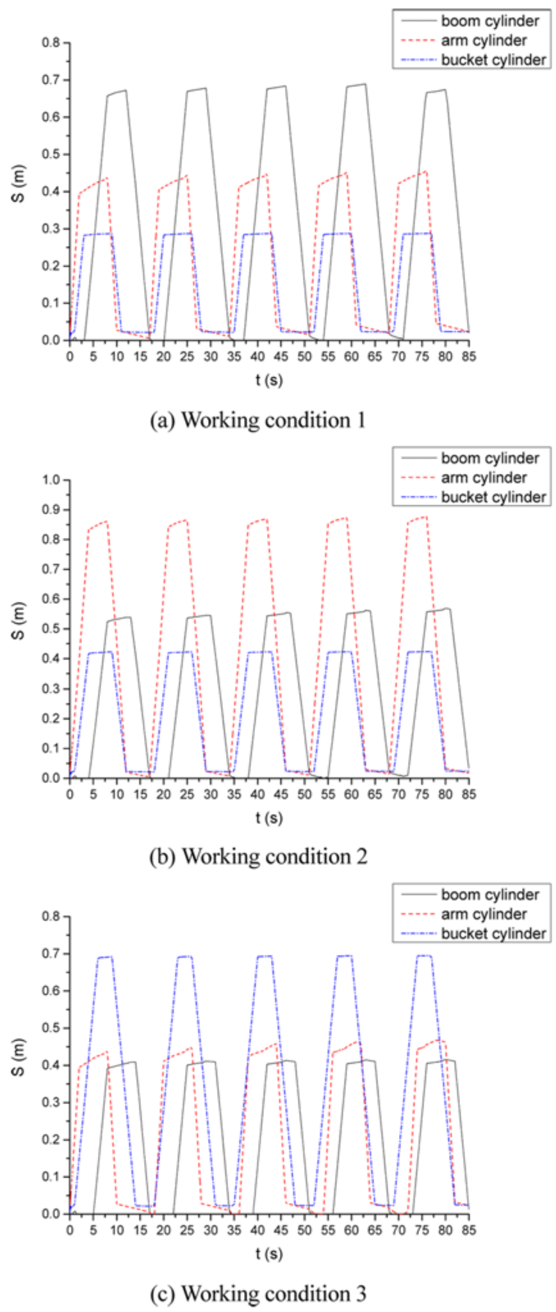

Fig. 17 Displacement of TCC piston rods in different working conditions

5. Energy Recovery Analysis in Different Working Conditions

Within this paper, three kinds of working conditions are simulated. Parameters of main components are shown in Table 1 and Table 6. According to the requirements of working conditions, the given control signals of pump displacement are shown in Fig. 16. In the figures, t is the time.

The piston rods' displacement (S) of each TCC over time t is shown in Fig. 17.

As the results of the simulation, the power of each pump (P) is shown in Fig. 18.

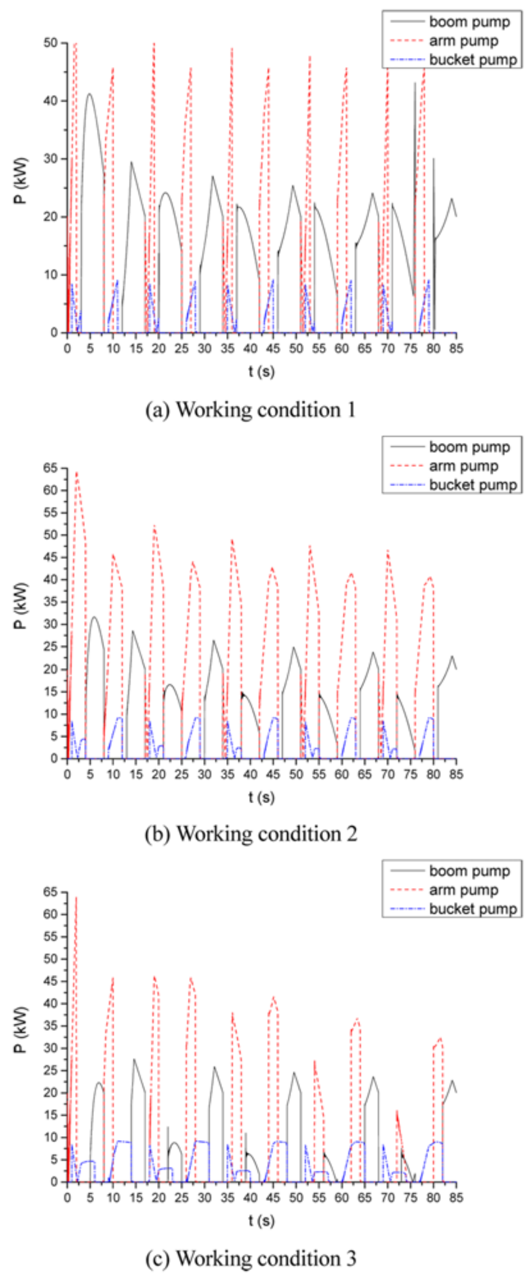

Fig. 18 Power of pumps in different working conditions

And the energy consumption of each pump (E) is shown in Fig. 19.

As a contrast, for a traditional hydraulic excavator without potential energy recovery under the same working conditions, the power of each pump is shown in Fig. 20.

The energy consumption of the pumps without energy recovery is shown in Fig. 21.

The comparison of the engine power between with and without potential energy recovery in different working conditions is shown in Fig. 22.

The comparison of the engine energy consumption between with and without potential energy recovery in different working conditions is shown in Fig. 23.

According to the simulation results, the maximum power of each pump and the engine under different working conditions with and

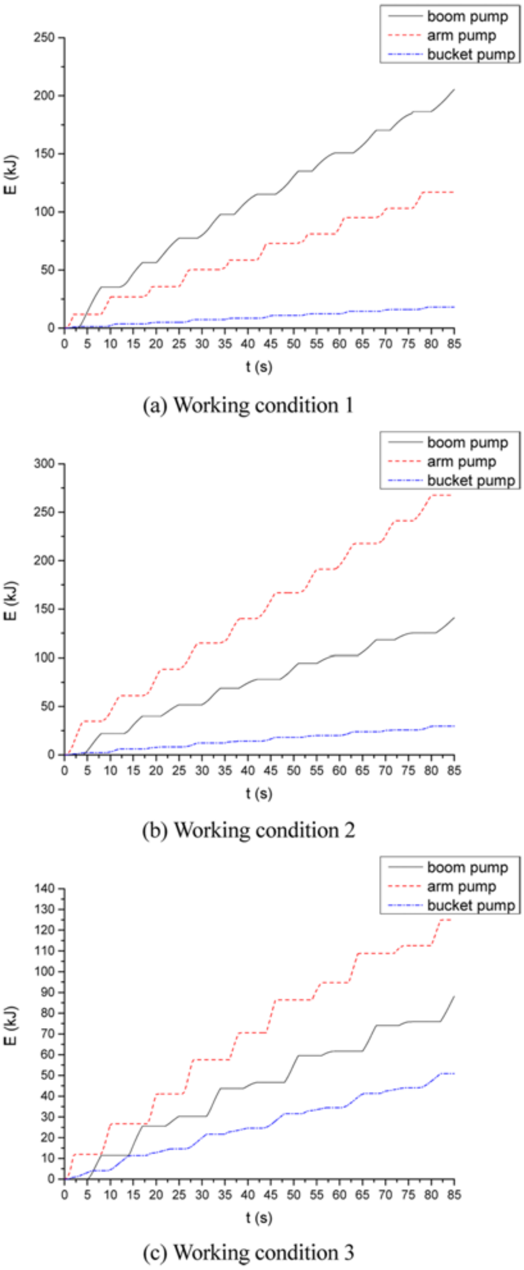

(a) Working condition 1

(b) Working condition 2

(c) Working condition 3

Fig. 19 Energy consumption of pumps in different working conditions

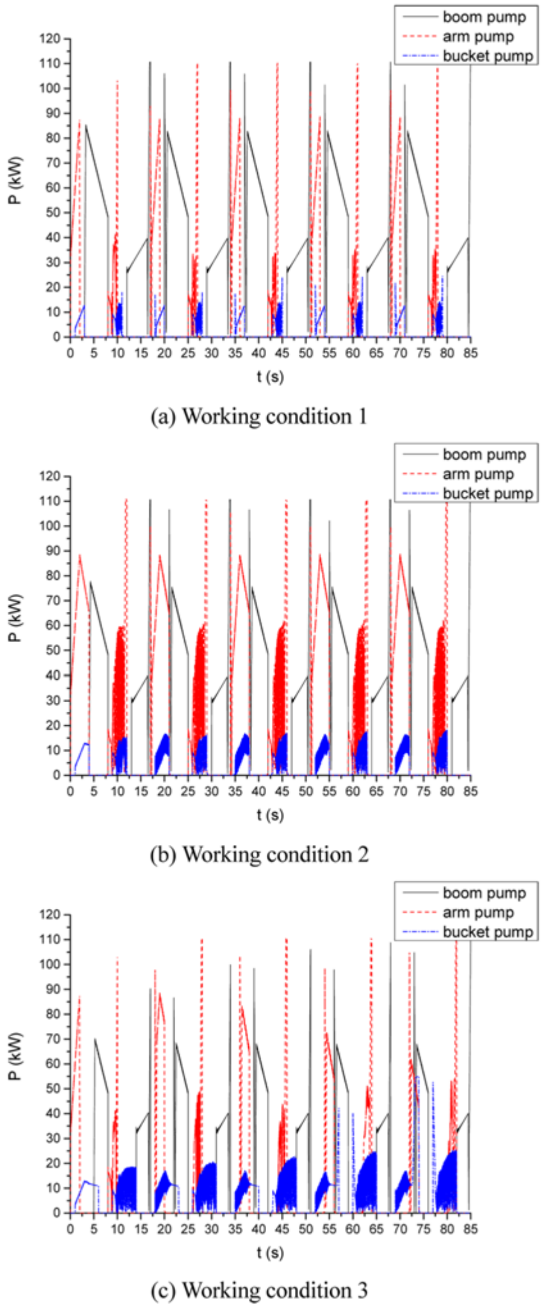

(a) Working condition 1

(b) Working condition 2

(c) Working condition 3

Fig. 20 Power of pumps without potential energy recovery in different working conditions

without energy recovery is summarized in Table 7.

The comparison between working conditions with and without potential energy recovery shows that the usage of TCCs and accumulators reduces the maximum power of the boom pump from about 110.0 kW to 43.2-27.6 kW, reduces the maximum power of the arm pump from about 110.0 kW to 64.2-46.2 kW, and reduces the maximum power of the arm pump from 18.8-55.0 kW to about 10.0 kW. Meanwhile, in the working condition without potential energy recovery, the maximum power of the engine is 114.5 kW, 128.8 kW and 170.8 kW, respectively. By contrast, the maximum power of the engine is about 65.0 kW with potential energy recovery.

Using TCCs and accumulators to recover potential energy of the mechanical arms of the excavator can reduce the maximum power of each pump to a great extent, and reduce the maximum power of the engine by 45.8% to 63.6%. The potential energy recovery system shows a more significant effect to reduce the maximum power of the boom and bucket pumps. But the effect of the arm pump is poorer.

The energy consumption of each pump and the engine under different working conditions with and without energy recovery within 5 work cycles is summarized in Table 8.

Table 8 shows that the usage of TCCs and accumulators reduces the energy consumption of the boom pump by 59.2-69.0%, reduces the energy consumption of the arm pump by 32.8-37.2%, and reduces the energy consumption of the bucket pump by 43.8-59.2%. Meanwhile, the energy consumption of the engine can be reduced by 49.9-57.3%.

On the basis of energy consumption simulation results, the potential

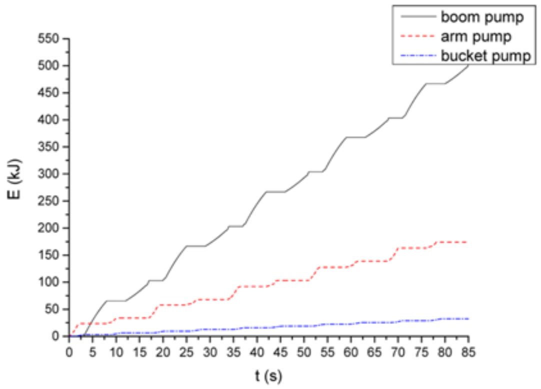

(a) Working condition 1

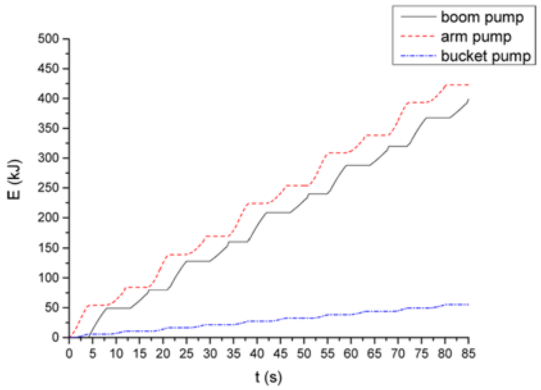

(b) Working condition 2

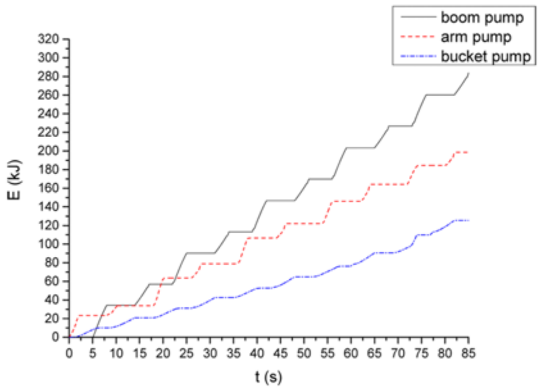

(c) Working condition 3

Fig. 21 Energy consumption of pumps without potential energy recovery in different working conditions

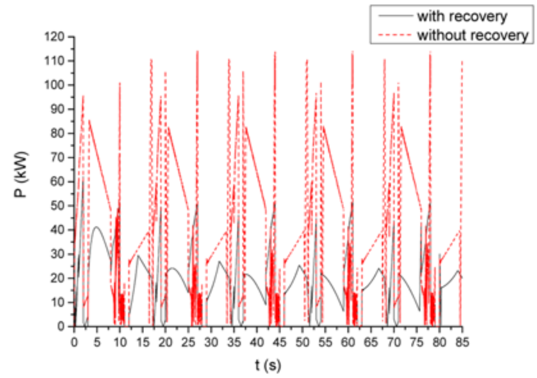

(a) Working condition 1

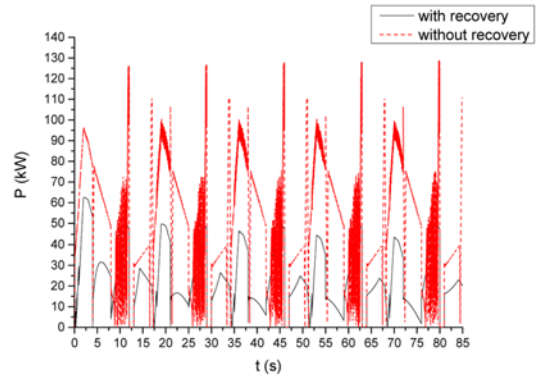

(b) Working condition 2

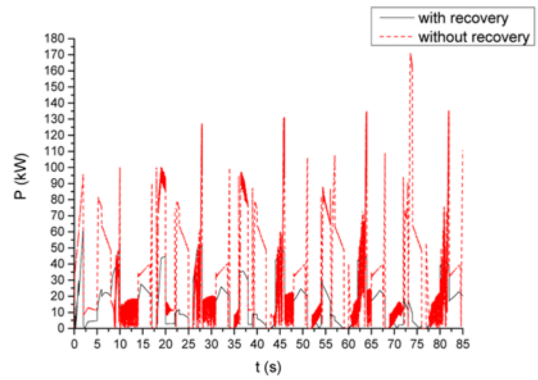

(c) Working condition 3

Fig. 22 Power of engine in different working conditions

energy recovery system has more significant effect to the boom. Since the direction of the boom cylinder load force is constant, the dead load is larger and the load fluctuation is smaller than the other two mechanical arms, and the energy recovery rate is higher. On the contrary, the direction of the arm cylinder load force is variable, and the load fluctuation is large, so the energy recovery rate is lower.

6. Conclusion

In this paper, a hydraulic hybrid excavator with potential energy recovery system is proposed. The system is based on the combination of TCCs and accumulators. The simulation results show that the increase of the accumulator volume weakens the control performance but heightens the stability of the system. However, the increase of the cross sectional area of the TCC strengthens the control performance, and influences the stability of the system. The increase of the accumulator volumes and the TCC diameters decrease the maximum power and energy consumption of the pumps and the engine, in general. But oversize accumulators and TCCs also bring disadvantages. So the selection of accumulator volume and TCC diameter should take installation space, engine power, load and expect energy recovery efficiency into account.

The potential recovery system reduces the maximum power and energy consumption in significant measure. The energy recovery rate is around 50% under different working conditions. Meanwhile, from the

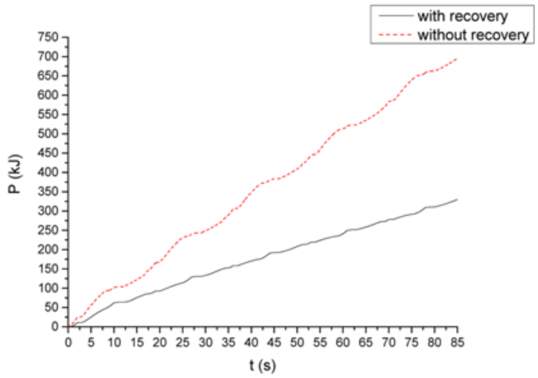

(a) Working condition 1

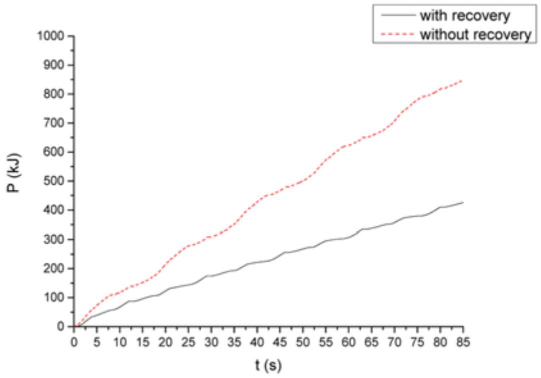

(b) Working condition 2

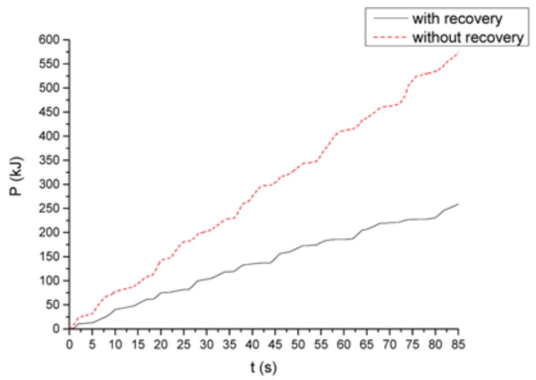

(c) Working condition 3

Fig. 23 Energy consumption of engine in different working conditions

comparison of energy recovery rate among boom, arm and bucket, the conclusion can be obtained that the recoverable energy of the boom is larger, and the recoverable energy of the bucket is smaller. The energy recovery rate of the boom is higher. Meanwhile, the energy recovery rate of the bucket and the arm is lower.

Moreover, a method to establish mathematical model of a hydraulic hybrid excavator is proposed in this work. With this method, dynamic characteristics and energy recovery characteristics of the system with different component parameters can be analyzed, which further contributes to parameter matching of the excavator. Also, simulation model is built using the mathematical model to acquire the energy recovery rate. In these respects, this work puts forward an approach to analyze excavator system performance and has some reference value for similar type of machineries.

Table 7 Maximum power of pumps and engine in different working conditions (Unit: kW)

	Energy recovery	Working condition 1	Working condition 2	Working condition 3
Boom pump	With	43.2	31.6	27.6
	Without	110.7	110.6	106.1
Arm pump	With	52.4	64.2	46.2
	Without	110.4	110.8	110.7
Bucket pump	With	9.2	9.8	11.5
	Without	24.7	18.5	55.0
Engine	With	62.1	68.5	62.2
	Without	114.5	128.9	170.8

Table 8 Energy consumption of pumps and engine in different working conditions (Unit: kJ)

	Energy recovery	Working condition 1	Working condition 2	Working condition 3
Boom pump	With	205	141	88
	Without	503	399	284
Arm pump	With	117	268	125
	Without	174	423	199
Bucket pump	With	18	30	51
	Without	32	55	125
engine	With	340	439	264
	Without	709	877	618

However, the mathematical model and the simulation model in this paper are idealized models, which rarely consider the efficiency or energy loss of each component. In order to reduce the calculation amount, some of the models are further simplified. Also, this work is at its early stage and the experiment validation condition is not mature. With the limitations mentioned above, future research will focus on mathematical model refinement and experiment validation.

ACKNOWLEDGEMENT

This work is supported by Foundation for Innovative Research Groups of the National Natural Science Foundation of China (Grant No. 51521064), and Independent Design Foundation for Key Scientific and Technological Innovation Team of Zhejiang Province, China (Grant No. 3013TD01).

REFERENCES

1. Taymaz, I. and Benli, M., "Emissions and Fuel Economy for a Hybrid Vehicle," Fuel, Vol. 115, pp. 812-817, 2014.

2. Salmasi, F. R., "Control Strategies for Hybrid Electric Vehicles: Evolution, Classification, Comparison, and Future Trends," IEEE Transactions on Vehicular Technology, Vol. 56, No. 5, pp. 2393-2404, 2007.

3. Hippalgaonkar, R. and Ivantysynova, M., "A Series-Parallel Hydraulic Hybrid Mini-Excavator with Displacement Controlled Actuators," Proc. of 13th Scandinavian International Conference on

Fluid Power, pp. 31-42, 2013.

4. Zimmerman, J., Hippalgaonkar, R., and Ivantysynova, M., "Optimal Control for the Series-Parallel Displacement Controlled Hydraulic Hybrid Excavator," Proc. of the ASME Dynamic Systems and Control Conference, pp. 129-136, 2011.

5. Sugimura, K. and Murrenhoff, H., "Hybrid Load Sensing–Displacement Controlled Architecture for Excavators," Proc. of the 14th Scandinavian International Conference on Fluid Power, pp. 20-22, 2015.

6. Erkkilä, M., Bauer, F., and Feld, D., "Universal Energy Storage and Recovery System-A Novel Approach for Hydraulic Hybrid," Proc. of 13th Scandinavian International Conference on Fluid Power, pp. 45-52, 2013.

7. Tikkanen S., To mmila H., "Hybrid pump drive," The Fourteenth Scandinavian International Conference on Fluid Power, Tampere: Tampere University of Technology, pp. 667-677, 2015.

8. Quan, Z., Quan, L., and Zhang, J., "Review of Energy Efficient Direct Pump Controlled Cylinder Electro-Hydraulic Technology," Renewable and Sustainable Energy Reviews, Vol. 35, pp. 336-346, 2014.

9. Jiang, J., Yu, A., and Shen, W., "The Review of Full Hydraulic Hybrid Excavator Based on Common Pressure Rail Network," Chinese Hydraulics and Pneumatics, Vol. 9, pp. 44-49, 2010.

10. Shen, W., Jiang, J., Su, X., and Karimi, H. R., "Control Strategy Analysis of the Hydraulic Hybrid Excavator," Journal of the Franklin Institute, Vol. 352, No. 2, pp. 541-561, 2015.

11. Shen, W. and Jiang, J.-H., "Analysis of Energy Recovery Efficiency of Hydraulic Hybrid Excavator," Journal of South China University of Technology, Vol. 40, No. 1, pp. 82-87, 2012.

12. Lin, S.-w. and Hua, H.-y., "Constant-Pressure-Network Readjustment Hydraulic System design And Energy Consumption Analysis for Excavators," Chinese Journal of Construction Machinery, Vol. 1, pp. 52-57, 2009.

13. Achten, P., Brink, T. V. D., Potma, J., Schellekens, M., Vael, G., and Innas, B., "A Four-Quadrant Hydraulic Transformer for Hybrid Vehicles," Proc. of 11th Scandinavian International Conference on Fluid Power, 2009.

14. Shen, W. and Jiang, J., "Analysis and Development of the Hydraulic Secondary Regulation System Based on the CPR," Proc. of International Conference on Fluid Power and Mechatronics, pp. 117-122, 2011.

15. Xiao, Y., Guan, C., and Lai, X., "Research on the Design and Control Strategy for a Flow-Coupling-Based Hydraulic Hybrid Excavator," Proceedings of the Institution of Mechanical Engineers, Part D: Journal of Automobile Engineering, Vol. 228, No. 14, pp. 1675-1687, 2014.

16. Andersen, T. O., Hansen, M. R., and Pedersen, H. C., "Regeneration of Potential Energy in Hydraulic Forklift Trucks," Proc. of Fluid Power Transmission and Control, pp. 302-306, 2005.

17. Huova, M., Laamanen, A., and Linjama, M., "Energy Efficiency of Three-Chamber Cylinder with Digital Valve System," International Journal of Fluid Power, Vol. 11, No. 3, pp. 15-22, 2010.

18. Stauch, C., Schulz, F., Bruck, P., Rudolph, J., and Weg, G. E., "Energy Recovery Using a Digital Piston-Type Accumulator," Proc. of the 5th Workshop on Digital Fluid Power. Tampere: Tampere University of Technology, pp. 57-73, 2012.

19. Sprengel, M. M. and Ivantysynova, M., "Investigation and Energetic Analysis of a Novel Hydraulic Hybrid Architecture for On-Road Vehicles," Proc. of 13th Scandinavian International Conference on Fluid Power, pp. 87-98, 2013.

20. Lin, X., Pan, S.-x., and Wang, D.-y., "Dynamic Simulation and Optimal Control Strategy for a Parallel Hybrid Hydraulic Excavator," Journal of Zhejiang University-Science A, Vol. 9, No. 5, pp. 624-632, 2008.

21. Bender, F. A., Kaszynski, M., and Sawodny, O., "Drive Cycle Prediction and Energy Management Optimization for Hybrid Hydraulic Vehicles," IEEE Transactions on Vehicular Technology, Vol. 62, No. 8, pp. 3581-3592, 2013.

22. Xiao, Q., "Control Strategy and Parameter Matching OF Hybrid System in Hydraulic Excavator," Zhejiang University, 2008.

23. Sinthipsomboon, K., Hunsacharoonroj, I., Khedari, J., Pongaen, W., and Pratumsuwan, P., "A Hybrid of Fuzzy and Fuzzy Self-Tuning PID Controller for Servo Electro-Hydraulic System," Proc. of 6th IEEE Conference on Industrial Electronics and Applications (ICIEA), pp. 220-225, 2011.

24. Li, W., Cao, B., Zhu, Z., and Chen, G., "A Novel Energy Recovery System for Parallel Hybrid Hydraulic Excavator," The Scientific World Journal, Vol. 2014, Article ID: 184909, 2014.

25. Zhang J., Li H. Y., Ma (B), et al, "Influence on Actuating Pressure Characteristics of Shift Clutch with Accumulator Regulating," Chinese Hydraulics and Pneumatics, Vol. 3, pp. 96-99, 2013.

26. Li, W., Cao, B., Zhu, Z., and Chen, G., "A Novel Energy Recovery System for Parallel Hybrid Hydraulic Excavator," The Scientific World Journal, Vol. 2014, Article ID: 184909, 2014.